National Aeronautics and Space Administration

Orbital Debris Quarterly News

Volume 27, Issue 4
October 2023

Inside...

A publication of the NASA Orbital Debris Program Office (ODPO)

ISS Maneuvers to Avoid Potential Collisions Twice in August 2023

The International Space Station (ISS) performed a Predetermined Debris Avoidance Maneuver (PDAM) on 06 August 2023 at 02:03 GMT to mitigate a projected high-risk conjunction with Cosmos 1408 debris (International Designator 1982-092BZV, U.S. Satellite Catalog Number 52808). This small fragment was created by the November 2021 anti-satellite test on Cosmos 1408 by the Russian Federation (ODQN vol. 26, issue 1, March 2022, pp. 1-5). The 83P *Progress* vehicle thrusters were again used to perform a standard 0.3 m/s posigrade maneuver. ISS apogee and perigee altitudes were raised by 0.73 km and 0.40 km, respectively.

A second PDAM was conducted on 24 August 2023 at 15:00 GMT to avoid a high-risk conjunction with *Fengyun*-1C (FY-1C) debris (1999-025DPV, Catalog Number 35213). This debris was created by the January 2007 anti-satellite test on FY-1C by the People's Republic of China (ODQN vol. 11, issue 2, April 2007, pp. 2-3). The *Zvezda* Service Module's main engines were used to perform a standard -0.3 m/s (retrograde) maneuver. ISS apogee and perigee altitudes were lowered by 0.18 km and 1.34 km, respectively. Both the timing of the PDAM and its retrograde direction were chosen to minimize the impact of the PDAM upon *Progress* 85P, the SpaceX Crew-7 vehicle, and the *Soyuz* 69S departure and 70S launch operations.

These PDAMs are the 36th and 37th collision avoidance maneuvers conducted by the ISS against tracked objects since 1999. ♦

Derelict Cosmos Communications Spacecraft Breaks Up in June 2023

The 18th Space Defense Squadron (18 SDS) of the U.S. Space Force has announced the breakup of the Soviet-era Cosmos 2143 communications spacecraft (International Designator 1991-033A, U.S. Satellite Catalog Number 21299). After approximately 32 years on-orbit, the spacecraft experienced a breakup at 06:49 GMT on 29 June 2023. At that time, the apogee altitude, perigee altitude, and inclination of the spacecraft were approximately 1416 km x 1398 km, and 82.6° respectively. The breakup occurred at an altitude of approximately 1400 km. The dry mass of the small spacecraft was approximately 225 kg. Six fragments, in addition to the parent body, are cataloged; these are international designator piece tags H-N and catalog numbers 57720-25. These are portrayed as a Gabbard diagram in the figure.

Cosmos 2143 was a member of the *Strela-3* store-dump communications constellation and

continued on page 2

June Breakup

continued from page 1

was a payload of a sextuple launch (colloquially referred to as a "six pack") aboard an SL14/F-2/*Tsyklon-3* launch vehicle. The eponymous *Strela-3* bus is believed to be identical to that of the Cosmos 1691 (U.S. Satellite Catalog) or Cosmos 1695 (Russian cataloging nomenclature) spacecraft that fragmented on 22 November 1985 after only 43 days on-orbit [1]. A joint Russian and American investigation identified the high-pressure (100 atm) NiH_2 battery as the likely root cause of that breakup event [2]. Other battery-related breakup events in low Earth orbit occurred after less than one year on-orbit, so the attribution of the inactive Cosmos 2143 event to a battery-related fragmentation would be unique but provided the limited inventory of stored energy aboard these small spacecraft, the high-pressure battery assembly cannot be excluded as a possible root cause in this case.

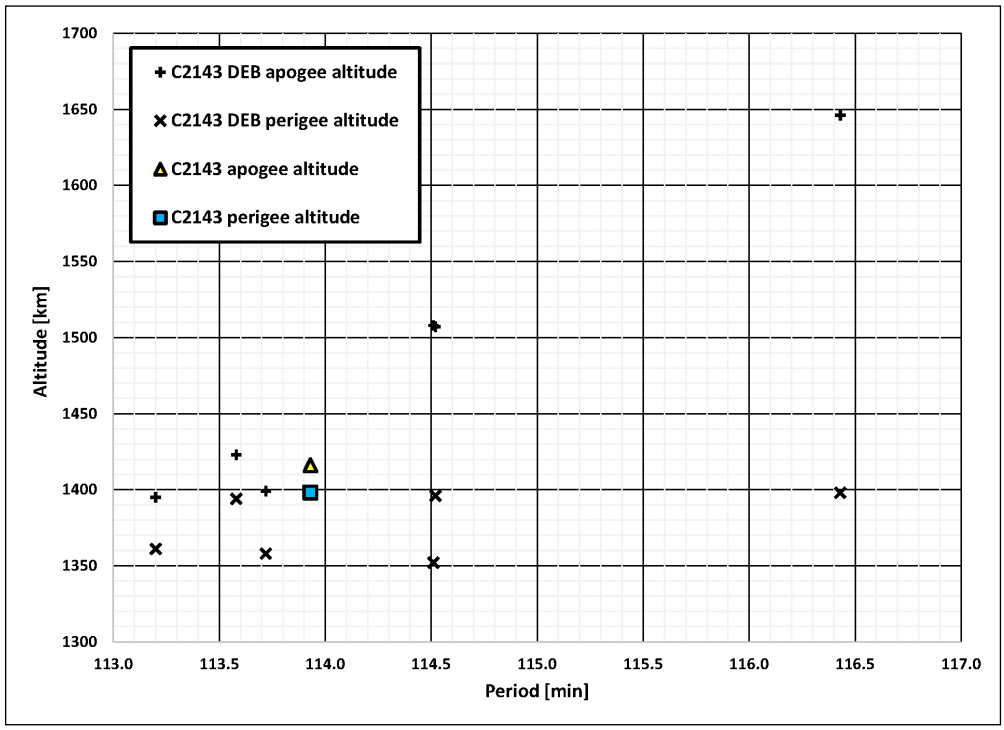

Cosmos 2143 debris ensemble at an epoch of 29 August 2023. The maximum change in inclination is 0.43° and maximum change in period is 2.5 minutes.

References

1. Anz-Meador, P., *et al*. History of On-orbit Satellite Fragmentations, 16th ed., NASA TP-20220019160, (December 2022).

2. Johnson, N.L., *et al*. "History of Soviet/Russian Satellite Fragmentations – A Joint US-Russian Investigation," p. 12, (October 1995). ♦

Gene Stansbery, Former NASA Program Manager for Orbital Debris, Passes

Mr. Eugene (Gene) Stansbery, NASA Program Manager for the Orbital Debris Program Office (ODPO) from 2006 to 2017, passed away on 11 August 2023. During his 30 years supporting the ODPO, Gene specialized in ground-based and *in-situ* debris measurement activities. As the ODPO Program Manager, Gene conceived, conducted, and directed research involving all aspects of orbital debris research, risk assessments, and mitigation. During his career, Gene authored or co-authored over 200 papers, reports, proceedings, book chapters, as well as innumerable internal studies and presentations.

As the ODPO Measurement Lead, Gene led development of the Haystack radar project to statistically characterize sub-centimeter debris in low Earth orbit (LEO) and contributed significantly to the Haystack Auxiliary (HAX) radar's development, commissioning, and use in characterizing debris in the centimeter size range. He also served as co-investigator for the Orbital Debris Radar Calibration Spheres (ODERACS) payload and principal investigator for ODERACS II, which deployed spheres and dipoles to verify calibration of Haystack and other radars and optical

continued on page 3

Stansbery Passes

continued from page 2

telescopes.

In concert with other ODPO staff members, he facilitated optical measurements of the near Earth and deep space regions for surveys and special projects, particularly those efforts using the Department of Defense's Ground-based Electro-optical Deep Space Surveillance (GEODSS) instruments, and was a strong advocate of optical measurement programs, including the ODPO's long-running observation campaigns using the 0.6-m Michigan Orbital Debris Survey Telescope (MODEST) located at the Cerro Tololo Inter-America Observatory and 6.5-m Magellan telescopes located at the Las Campanas Observatory, both in Chile. As a possible alternative or adjunct to radars, Gene also supported the development and deployment of the ODPO Liquid Mirror Telescope in New Mexico, USA, for observing LEO debris.

In 2000, Gene conceived the idea of a meter-class autonomous telescope (MCAT) and spent the next 15 years persistently shepherding the MCAT project through development and its commissioning on Ascension Island in June 2015. To recognize Gene's many contributions to MCAT, the ODPO dedicated and officially renamed the meter-class telescope to the Eugene Stansbery MCAT (ES-MCAT) when he retired from NASA. ES-MCAT continues to serve as the primary source of ODPO optical measurements of the orbital debris environment for improvements to ODPO's environmental models.

On 30 June 2011, Gene received the NASA Exceptional Service Medal for "dedication, leadership, and creativity in establishing international preeminence in orbital debris observation, measurement, analysis, and modeling at NASA". His many accomplishments are recognized not only by the ODPO, but also by the domestic and international orbital debris community.

Gene will be sorely missed by many who have had the honor of working with him through the decades. ♦

PROJECT REVIEW

HUSIR Radar Measurements of the Orbital Debris Environment: 2022

J. ARNOLD AND A. MANIS

The NASA Orbital Debris Program Office (ODPO) relies on radar measurements to characterize the distribution of orbital debris (OD) in low Earth orbit (LEO) smaller than those typically tracked and cataloged by the U.S. Space Command's Space Surveillance Network (SSN), but large enough to pose a threat to operational satellites, robotic missions, and human spaceflight. The dynamic nature of the OD environment requires ongoing monitoring. This review article gives an overview of the OD radar data collected by the Haystack Ultrawideband Satellite Imaging Radar (HUSIR) during calendar year (CY) 2022 and outlines significant changes to the OD environment compared with CY2021 (ODQN, vol. 26, issue 3, September 2022, pp. 3-5) and [1] including the effects of a direct-ascent anti-satellite (ASAT) test conducted by Russia against its Cosmos 1408 (C1408) satellite (ODQN, vol. 26, issue 1, March 2022, pp. 1-5).

HUSIR serves as the ODPO's primary source of OD radar data. The data collected by HUSIR is used to statistically sample objects in LEO and LEO-crossing orbits, using these results to improve models that estimate the risk to operational missions. For OD radar data collection, HUSIR operates in a beam park mode, where the antenna is pointed at a fixed azimuth and elevation angle relative to the horizon and objects are detected as they randomly pass through the radar beam. HUSIR operates in three main pointing geometries employed by the ODPO; 75° elevation, due East (75E); 20° elevation, due South (20S); and 10° elevation, due South (10S). The bulk of the data is collected at the 75E pointing, which provides information on orbits with an inclination of roughly 40° to 140°, assuming a circular orbit.

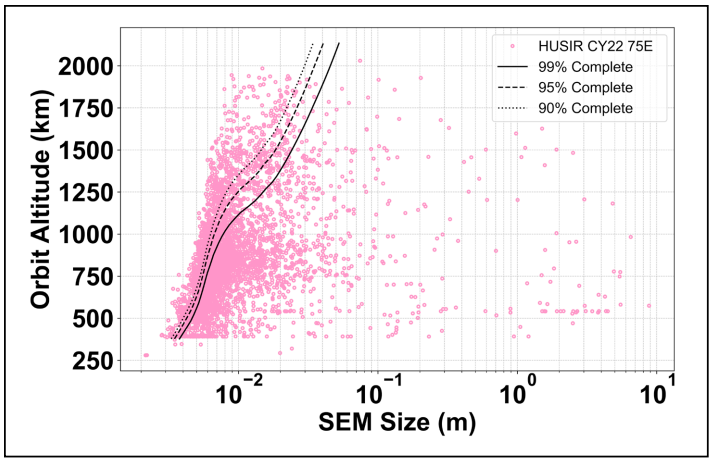

Figure 1. Orbit altitude versus SEM size for HUSIR CY2022 75E data at 10.1 GHz with 99%, 95%, and 90% altitude-dependent completeness curves.

Debris sizes are estimated from the measured radar cross sections (RCS) in conjunction with NASA's size estimation model (SEM) [2]. The RCS of an object is calculated from the power of the reflected signal relative to the transmitted signal and the range of the object. The completeness size of objects that can be detected by HUSIR is a function of altitude and is determined by the radar sensitivity, latitude, and pointing geometry. While average sensitivity varies from year-to-year,

continued on page 4

HUSIR Measurements

continued from page 3

historically, HUSIR has been able to sample the OD environment down to approximately 5.5 mm to an altitude of up to 1000 km. Figure 1 shows a plot of orbit altitude versus SEM size for objects detected in CY2022 with curves representing the altitude-dependent completeness sizes – that is, the lower bounds for which we are able to see 90%, 95%, and 99% of objects larger than those cut-off sizes. For CY2022, the completeness sizes at 1000 km are 6.2 mm, 6.5 mm, and 7.2 mm, for 90%, 95%, and 99% completeness, respectively. These sizes are slightly larger than the nominal historical limit due to a reduction in sensitivity during most of CY2022 as compared to previous years due to hardware-related changes in transmit power.

In previous years, the OD waveform used by HUSIR was centered at a frequency of 10 GHz. Over time, radio frequency interference (RFI) at 10 GHz became more pervasive, significantly reducing the amount of useable data. The Massachusetts Institute of Technology/Lincoln Labs (MIT/LL) was not able to determine the source of this interference; however, 10 GHz is a commonly used frequency for radiolocation, wireless broadband, and amateur radio. To lessen the impact of RFI, MIT/LL developed a new waveform with a center frequency of 10.1 GHz in CY2020. To validate the performance of this new waveform, data was collected at both the 10 GHz and 10.1 GHz center frequencies in CY2020 and CY2021. The 10.1 GHz waveform was shown to produce data comparable to the 10 GHz waveform, and the 10.1 GHz waveform has been used exclusively since 01 October 2021 [1]. The 10.1 GHz data experienced no RFI contamination in CY2021 or CY2022; however, HUSIR data continues to be monitored by the ODPO for RFI in case new sources of background interference emerge.

Because the beam park mode does not permit objects to be tracked over long distances, it is difficult to precisely determine the orbits of detected objects. The inclinations of objects traveling through the beam can instead be estimated using the measured range along with the range-rate, or Doppler velocity, if a circular orbit is assumed. This assumption allows the conversion of the data from range and range-rate to orbit altitude and Doppler inclination, as shown in Figure 2. Presented this way, several debris families can be identified, with the largest being the sun-synchronous family of orbits clustered around the dashed

continued on page 5

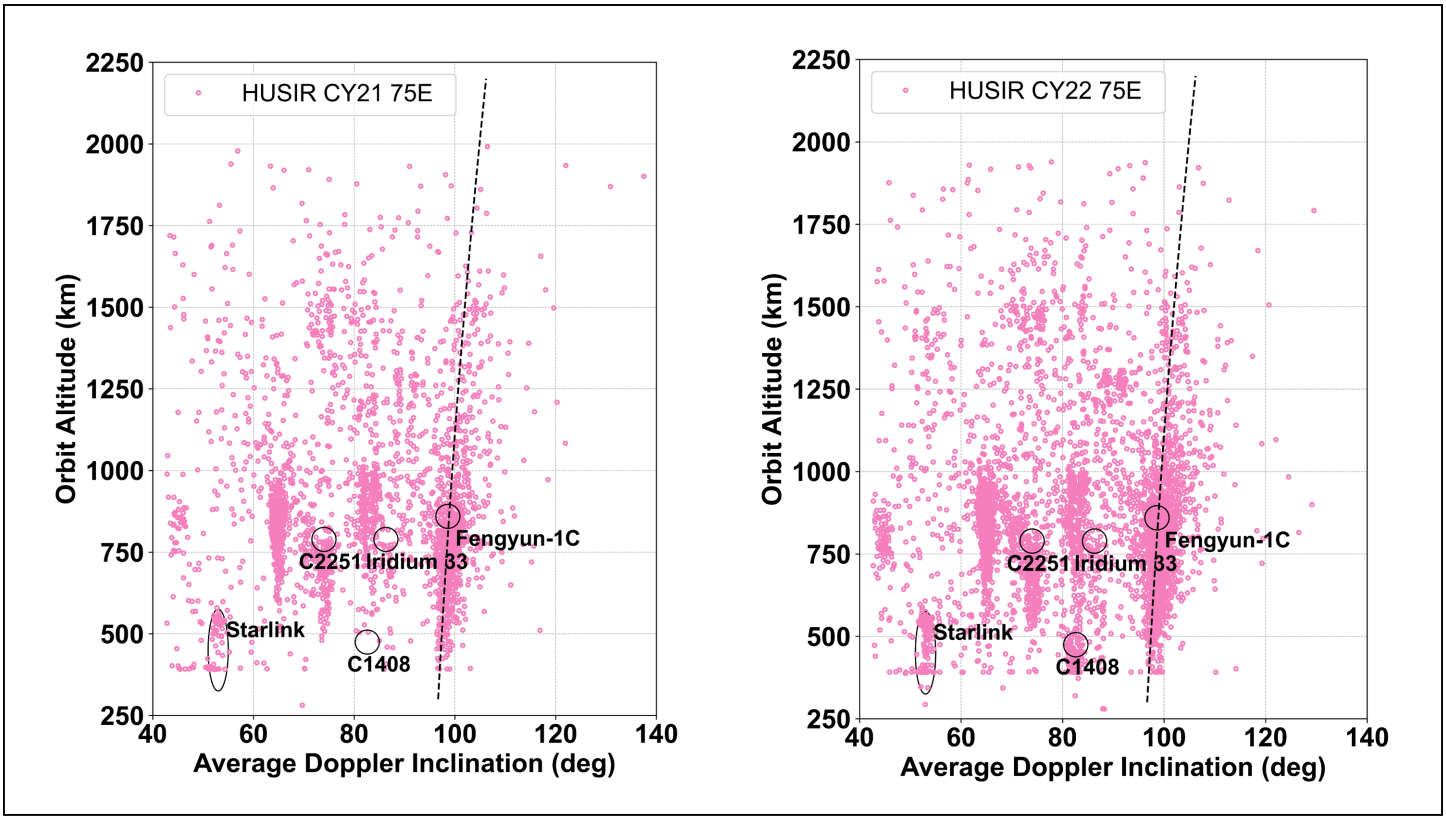

Figure 2. (left) Conversion of HUSIR CY2021 and (right) CY2022 range and range-rate measurements into orbit altitude and Doppler-derived inclination. The sun-synchronous condition, assuming a circular orbit, is indicated by the dashed black line. Notable debris clouds due to fragmentation events are highlighted with black circles, while detections associated with the Starlink constellation are emphasized by the black oval near 50° Doppler inclination.

HUSIR Measurements

continued from page 4

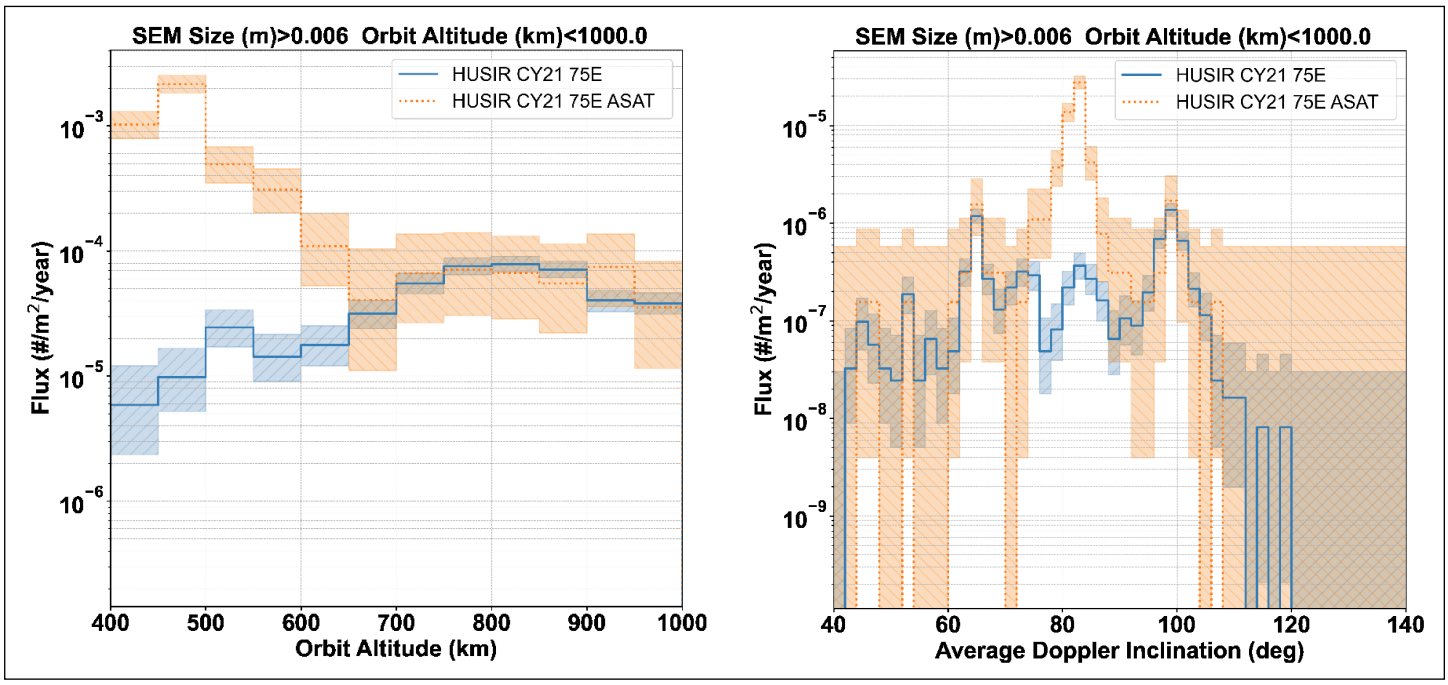

Figure 3. (left) Histograms of surface area flux versus altitude and (right) inclination of the special HUSIR ASAT test observations as compared to the background environment measured in CY2021, where flux is limited to objects 6 mm and larger and altitudes less than 1000 km. The shaded regions correspond to the 2σ-Poisson confidence intervals.

black line indicating the sun-synchronous inclinations. Several notable on-orbit fragmentation events are also highlighted in Figure 2 with black circles, including the recent C1408 ASAT test. The circles are centered on the altitude and inclination of the parent body at the time of the event. Additionally, a black ellipse outlines detections associated with the Starlink satellite constellation at approximately 53° inclination and 550 km altitude. Overall there were more detections at 75E in CY2022 (4741) than CY2021 (2651) due to a proportionally larger number of hours of data retained after RFI removal in CY2022.

On 15 November 2021, the C1408 ASAT test generated at least 1500 debris fragments trackable by the SSN as well as many smaller debris fragments. Within a day of the C1408 fragmentation event, the ODPO initiated a 25-day study to monitor the evolution of the resulting debris cloud [3]. For this study, the HUSIR observation windows were chosen that corresponded to the predicted times when the debris cloud would pass through the radar beam. Due to the timing of the ASAT test late in 2021, the C1408 fragments were not captured in the background CY2021 data.

A useful metric for recognizing changes to the OD environment using the HUSIR radar data is the surface area flux, or number of objects detected within the surface area of the radar beam per unit time. Figure 3 demonstrates how the ASAT debris cloud has a very distinct surface area flux distribution in altitude and inclination compared with the debris background from CY2021. In Figure 3, flux is limited to sizes larger than 6 mm, the approximate size at which HUSIR measurements are complete at 1000 km altitude and is lower for CY2021. In altitude, the highest flux occurred in the 450 km to 500 km altitude bin, corresponding to the altitude at which the breakup occurred. The flux is also elevated above background levels down to 400 km, the lower limit for HUSIR observations, and up to 650 km altitude. In inclination, the highest flux was observed at 82° to 84°, corresponding to the orbital inclination of C1408 prior to its destruction, with flux elevated above background levels from 74° to 88° inclination.

Figure 4 shows histograms of surface area flux binned by altitude and inclination for all CY2021 and CY2022. Here, the fluxes are limited to sizes larger than 7.2 mm, the approximate completeness size for CY2022. The effect of the C1408 ASAT test fragments, as well as increased Starlink traffic, is apparent in the broad year-over-year increase in flux at altitudes of 400 km to 600 km (Figure 4, left-hand image). The C1408 debris cloud is centered at roughly 82.6° inclination and the Starlink orbits are clustered at roughly 53° in inclination. Increases in debris flux at these distinct inclinations can be noted in Figure 4's right-hand image.

HUSIR continues to provide the ODPO with critical information about the evolution of the OD environment for small debris at LEO altitudes. This information includes monitoring debris clouds generated by fragmentation events such as the

continued on page 6

HUSIR Measurements

continued from page 5

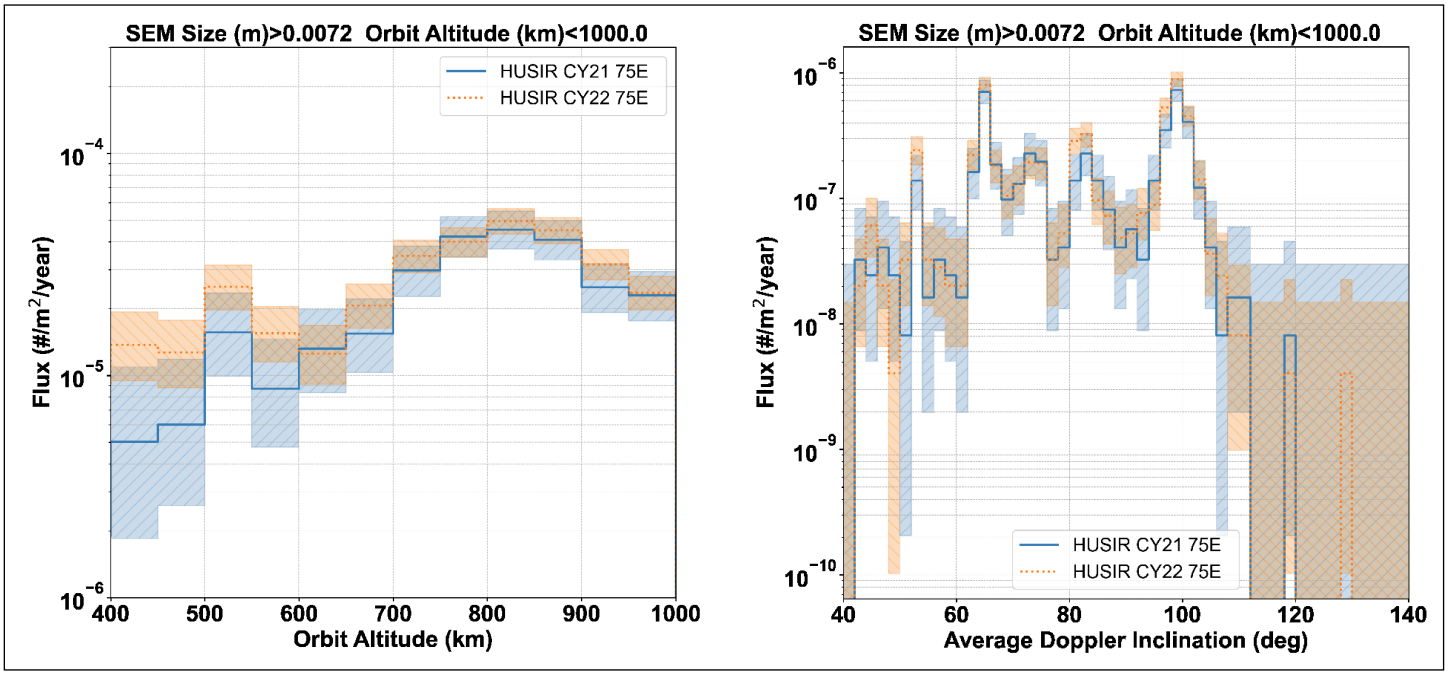

Figure 4. (left) Histograms of debris surface area flux as a function of altitude and (right) average Doppler inclination, where flux is limited to objects 7.2 mm and larger and altitudes less than 1000 km. The shaded regions correspond to the 2σ Poisson confidence intervals.

C1408 ASAT test that occurred just prior to the start of CY2022. The subsequent changes to the debris environment are readily noticeable when comparing HUSIR data from CY2022 versus CY2021 and highlight the need for continued observations to capture the dynamic effects of such events and provide timely data for updating OD environment models.

References

1. Murray, J. and Matney, M. "HUSIR Radar Measurements of the Orbital Debris Environment: 2021," NASA/TP 20230008344, (2021).

2. Xu, Y.-L. and Stokely, C. "A Statistical Size Estimation Model for Haystack and HAX Radar Detections," 56th International Astronautical Congress, Fukuoka, Japan, (2005).

3. Murray, J., *et al*. "Observations of Small Debris from the Cosmos 1408 Anti-satellite Test using the HUSIR and Goldstone Radars," Advanced Maui Optical and Space Surveillance Technologies Conference (AMOS), (2022). ♦

Thirty Years Later: A Look Back at the 1993 JSC Perseid Stormwatch Center

M. CINTALA, P. ANZ-MEADOR, M. MATNEY, AND W. COOKE

In late 1992, the comet 109P/Swift-Tuttle returned to the inner Solar System on its 133-year orbit. Because this comet is known to be the parent body of the annual Perseid meteor shower, there were some predictions [1] that the August 1993 Perseid meteor shower might show an unusual outburst in rate and perhaps become a meteor storm, with rates of visual meteors potentially reaching greater than 100,000 per hour. Fainter meteors would perhaps be even more abundant. Under such conditions, the probability of meteoroids impacting orbiting spacecraft would undergo a drastic increase. At that time the confidence with which these probabilities could be assessed was uncomfortably low, due to the overall poor understanding of the mechanics of meteoroid-stream formation. Thus, the only viable means of evaluating the potential threat to orbiting assets — not the least of which would have been the shuttle orbiter Discovery on Mission STS-51 (Figure 1) — would be to monitor the evolution of the Perseid shower in real time. That would at least permit an estimate of the rate of change of the meteoroid flux and its absolute value — literally hours before the scheduled launch of STS-51.

On Friday, 06 August 1993, members of the Johnson Space Center (JSC) Solar System Exploration Division were asked by

continued on page 7

Perseid Stormwatch Center

continued from page 6

Figure 1. STS-51 Mission Patch

NASA management to form a "Perseid Stormwatch Center," with the objective of acting as a clearinghouse for reports from around the world. That information would then be synthesized into a coherent assessment of Perseid activity and distributed through electronic media to the entire community of reporting observers, various satellite owners and operators, and other government agencies mandated to monitor the near-Earth environment. More directly, the status of the Perseid shower would be summarized for the STS-51 Mission Management Team (MMT) during their prelaunch meeting.

Stormwatch Center operations began less than three days later at 13:00 GMT on Monday, 09 August, and continued until 17:00 GMT on Friday, 13 August, during which time the Center was staffed continuously. Activities centered primarily around collecting reports from sites around the world (including stations in Asia, Europe, Hawaii, and North America); disseminating the synthesized data as the incoming reports clarified the shower's temporal behavior-manifested by onset and visual meteor rates; and conducting observations with the 5 MHz Transportable Radar System located at JSC. The latter were supported by periods of visual observation from the field adjacent to the radar antenna.

Observations from most of western Europe were stymied by uncooperative weather, but the peak of the shower was visible to observers in Slovenia and southern France, who estimated a rate of 600 to 800 visual meteors per hour. Subsequent analysis conducted by the International Meteor Organization [2] indicated a peak zenithal hourly rate (ZHR) exceeding 300 at about 3h30m UT, with a peak full-width, half-max duration of approximately 2 hours. Figure 2 depicts Perseid activity from 11 August through 14 August. Although this ZHR was notably above the numbers for typical Perseid showers, it was roughly consistent with the 1991 and 1992 showers and orders of magnitude below the worst-case values. This information was transmitted to the STS-51 MMT, and the countdown proceeded, only to see the launch aborted at T-3 seconds because of an errant fuel-flow sensor in one of the orbiter's main engines. Discovery successfully launched a month later on 12 September, the only crewed NASA mission ever at risk of a schedule slip due to a meteoroid shower.

After the Perseids, interest grew in the expected 1999 Leonid meteor storm and the possibility that it would pose an enhanced spacecraft hazard. Marshall Space Flight Center (MSFC) scientists developed strong competencies during the Leonid activity from 1998 to 2002; however, it was NASA Headquarters' recognition of the importance of fostering an organic meteoroid center of expertise, based on the Columbia Accident Investigation Board findings, that led NASA to create the Meteoroid Environment Office (MEO) at MSFC in 2004 to address these risks for spaceflight.

The NASA MEO produces models for all meteoroid environments that pertain to spacecraft engineering and operations and makes measurements of the meteoroid environment in near-Earth space. More information on the applications for understanding the flux associated with the risk of meteoroids impacting spacecraft can be found at https://sma.nasa.gov/sma-disciplines/meteoroid-environments.

References

1. Rao, J. "Perseids 1993: The Big One?" WGN, the Journal of the IMO, vol. 21, no. 1, , pp. 110-21, (1993).

2. Rendtel, J. "Perseids 1993: A First Analysis of Global Data," WGN, the Journal of the IMO, vol. 21, no. 5, pp. 235-42, (1993). ♦

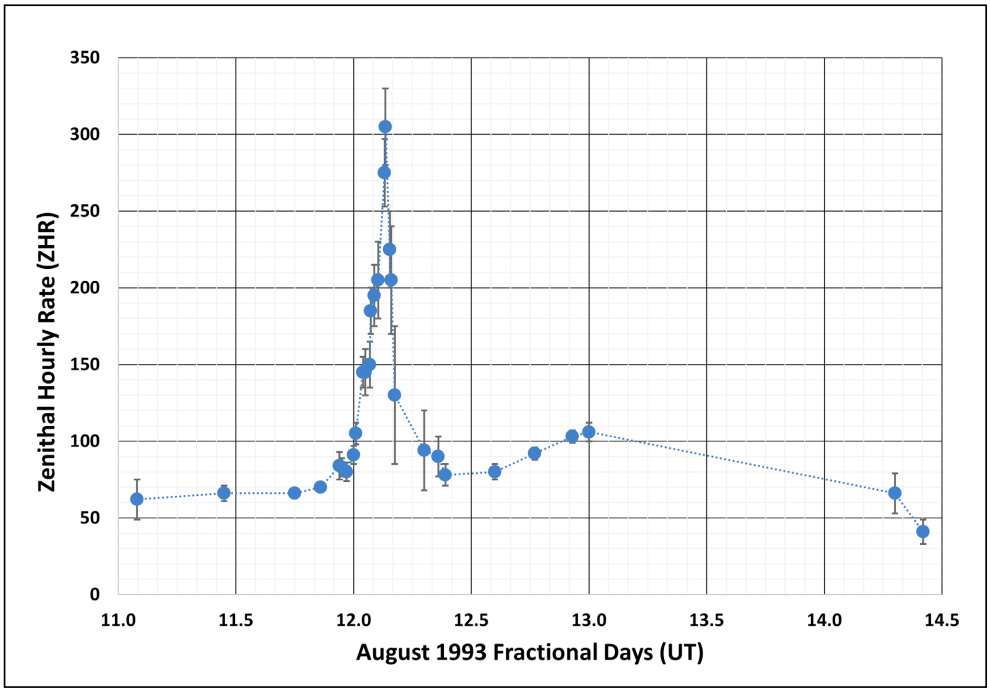

Figure 2. The computed post-event Zenithal Hourly Rate (ZHR) of the 1993 Perseid shower (after Ref. 1, Table 2). Poisson one sigma uncertainties are plotted with the time-dependent rate.

The Second International Orbital Debris Conference (IOC II) will convene December 4–7, 2023 in Sugar Land, Texas. The conference goal is to highlight orbital debris research activities in the United States and to foster collaborations with the international community. The four-day conference will cover all aspects of orbital debris research, operations and mission support, environment management, and other related activities. Registration and hotel information for the conference is still open, and the link to the program and accepted abstracts are all available at https://www.hou.usra.edu/meetings/orbitaldebris2023/. ♦

CONFERENCE ABSTRACT FROM THE NASA ORBITAL DEBRIS PROGRAM OFFICE AND HYPERVELOCITY IMPACT TECHNOLOGY TEAM

The 24th Advanced Maui Optical and Space Surveillance Technologies Conference, 19-22 September 2023

Orbital Debris Shape Effect Investigations for Mitigating Risk

H. COWARDIN, E. CHRISTIANSEN, M. MATNEY, J. MILLER, B. DAVIS, C. CRUZ, J. SEAGO, A. KING, J. OPIELA, AND A. MANIS

NASA's Orbital Debris Program Office (ODPO) and Hypervelocity Impact Technology (HVIT) team have coordinated to better understand the risks to upper stages and spacecraft from non-spherical orbital debris. It is well understood that fragmentation (collision or explosion) events in orbit produce fragments of various materials, sizes, and shapes. To further characterize these parameters, the ODPO is developing the next-generation Orbital Debris Engineering Model (ORDEM) version 4.0 to include orbital debris shape distributions. Ground-based assets, such as radar and optical sensors, can provide size estimates and some insight into material based on radar return or optical filter photometry/spectroscopy, respectively. Characterizing an object's shape requires more laboratory analyses to infer how shape affects these measurements. More importantly, in addition to size and material/density, the shape of fragments in orbit will alter the ballistic limit equations used in orbital debris risk assessments with NASA's Bumper Code. The ODPO plans to release ORDEM 4.0 in the coming years.

Performing ground-based laboratory impact tests on high-fidelity spacecraft mockups provides the means to directly measure size, mass, material/density, and shape of fragments, all key parameters needed to characterize real-world break up events. The DebriSat test, the results of which are provided, showcases the details of this type of experiment. The goal of this collaborative research between the ODPO and the HVIT team is to include a shape parameter in the environmental and breakup models used to assess risk for various space structures.

This paper examines ground-based laboratory impact tests and the associated fragment shape categories. Provided these defined shapes, the approach is simplified by assuming a right circular cylinder (RCC) approximation with varying length-to-diameter ratios. Highlights of impact tests conducted by the HVIT team using non-spherical projectiles based on the RCC approximation are presented. Hydrocode simulations have also been performed to expand on the complexity of variations with non-spherical projectiles. Lastly, ray-tracing simulations of various RCCs of known material are provided to support the ongoing research on optical reflectance distributions with known

AMOS - Cont.

continued from page 8

shapes and to highlight how this may modify the current optical size estimation model. The status and plan forward are outlined for NASA's orbital debris shape effect investigation using a multidisciplinary approach by the ODPO and the HVIT team. ♦

CONFERENCE REPORT

24th Advanced Maui Optical and Space Surveillance Technologies Conference

The 24th Advanced Maui Optical and Space Surveillance Technologies (AMOS) Conference was held in hybrid format 19-22 September 2023. This year's record-breaking event hosted 1330 attendees with 251 virtual participants, including representatives from 25 countries. The opening keynote speaker was General B. Chance Saltzman, Chief of Space Operations, United States Space Force. Gen. Saltzman discussed the increased launch traffic; provided an overview on the mission statement for securing nations in, to, and from space; and spoke to the need for timely coordination and continuing coalitions – essential to support space domain awareness (SDA). Following the primary keynote address, Colonel Jeremy A. Raley, Director for Space Vehicles Directorate, Air Force Research Laboratory and Colonel Joseph R. Roth, Director of Innovation and Prototyping Acquisition Delta and Commander, Space Systems Commands Detachment 2, U.S. Space Force gave a joint talk on how artificial intelligence and machine learning can support SDA.

Dr. Diana Howard, Director of Commercial Space Policy, National Space Council provided a virtual keynote address on day two of the conference. Dr. Howard discussed the difficulties with implementing Space Policy Directive-3 due to lack of funding and the need for clearly defined roles in both government and the private sector. The next invited talk was given by Colonel Raj Agrawal, Commander, Space Delta 2-Space Domain Awareness. Col. Agrawal presented a high-level overview on Delta-2 and how he envisions utilizing SDA understanding for future opportunities and the mitigation of vulnerabilities to help secure national interests.

On the last day, a keynote address was provided by Elizabeth Pearce, a/g Director of Space Technology, Office of the Chief Technology Officer, Australian Space Agency. The presentation discussed the technological advancements Australia has made over the decades to support space situational awareness (SSA). The last keynote address was presented by Dr. Kelly Hammett, Director and Program Executive Officer for the Space Rapid Capabilities Office. Dr. Hammett discussed the history of the organization and highlights from recent successes that empower quick movement for technical advancements in support of securing the nation's interest.

This year also featured a presentation from Dr. Lindsay Millard, Principal Director for Space Technology, Office of the Under Secretary of Defense for Research and Engineering. The focus of the talk was on empowering defense space technology investment and the difficulty of predicting how technology will change the world.

After each keynote address, three panels were held that focused on SSA policy forums for the evolution of the commercial SSA data market, U.S. progress on civil SSA and space traffic management (STM), and moving from industry best practices to STM rules.

The Space Debris session, co-chaired by representatives from the NASA Orbital Debris Program Office (ODPO) and the University of Warwick, saw a variety of papers presented, including: small satellite experiment for increasing drag; space-based observations of plasma waves during conjunctions; estimating orbital debris mass via solar radiation pressure; the characterization of NaK from Soviet Radar Ocean Reconnaissance Satellite reactors; low Earth orbit population evolution modeling; Intelligence Advanced Research Projects Activity's Space Debris Identification and Tracking Program; statistical modeling for Kessler Syndrome; physical-economical model for space debris; statistical analysis of space debris surveys in high-altitude orbital regions; a space-based optical component for the European Space Agency's Verification of In-Situ Debris Optical Monitoring from Space Mission Mission; the distribution of relative accelerations in the vicinity of the geosynchronous orbit satellites; uncertainty in orbital lifetime estimation after post-mission disposal; and refining active debris removal strategies. The ODPO gave an oral presentation on "Orbital Debris Shape Effect Investigations for Mitigating Risk," a joint research effort between the ODPO and NASA's Hypervelocity Impact Technology Team.

The next AMOS conference is scheduled for 17-20 September 2024. ♦

The ODPO announces an opening for a postdoctoral fellow via the NASA Postdoctoral Progam. This position would support an *in-situ* sensor in development to characterize the small (millimeter-sized) orbital debris environment in low Earth orbit. Opportunities are available to support the development of the sensor and provide oversight and analyses that directly support future flight missions. For more information on this position, please see the request.

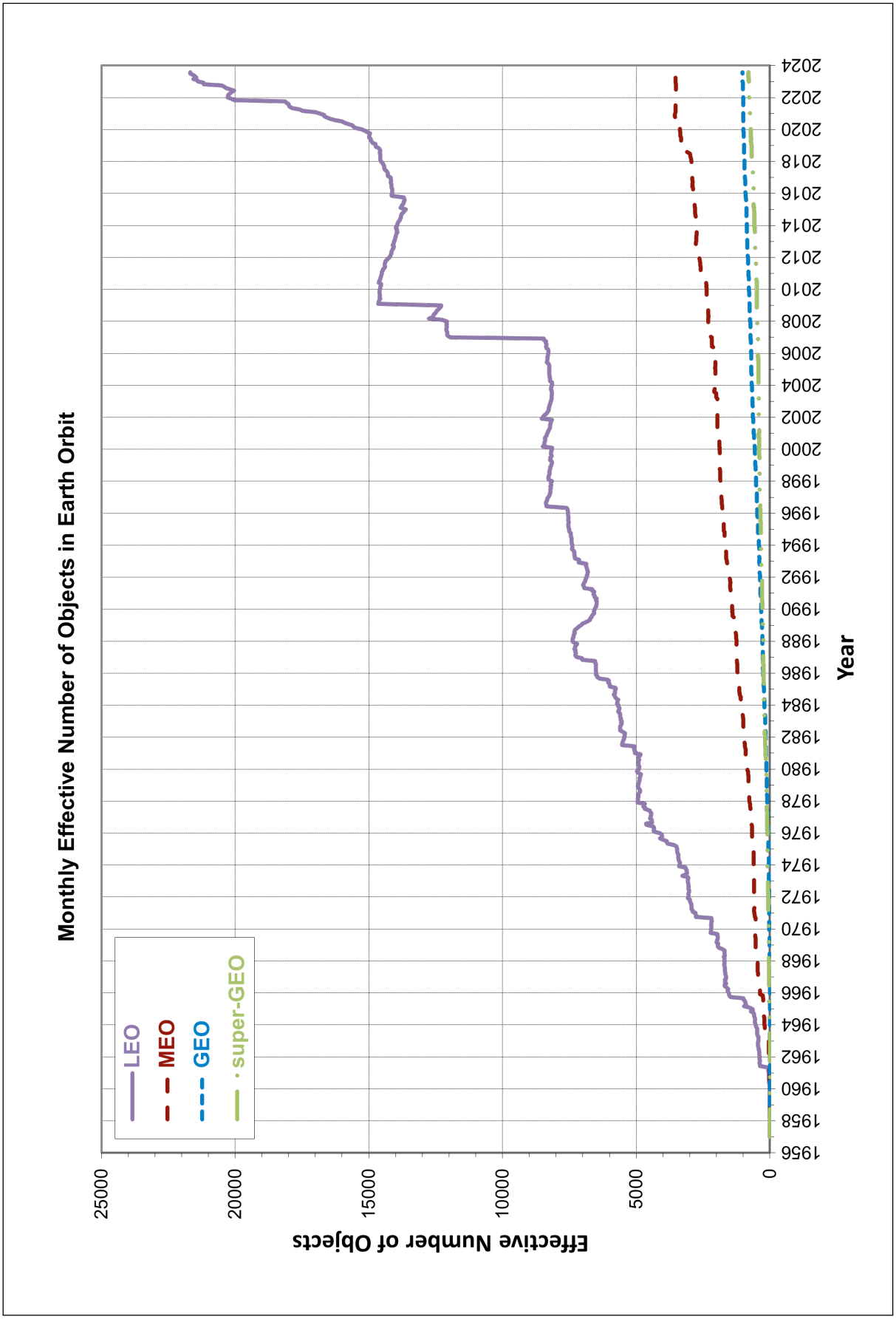

Monthly Effective Number of Objects in Earth Orbit by Orbital Regime cataloged by the U.S. Space Surveillance Network. This chart displays the number of all objects in Earth orbit officially cataloged by the U.S. Space Surveillance Network. Low Earth orbit (LEO) includes resident space objects (RSOs) with altitudes within or crossing below 2,000 km; medium Earth orbit (MEO) RSOs with altitudes within or crossing the range from 2,000 km to 35,586 km; geosynchronous orbit (GEO) RSOs with altitudes within or crossing the range from 35,586 km to 35,986 km; and the remainder with altitudes within or crossing the range from 35,986 km to 600,000 km, referred to as Super-GEO. "Effective" number sums the fraction of each orbit that falls within the specified ranges. Cataloged objects without available orbital elements are excluded.

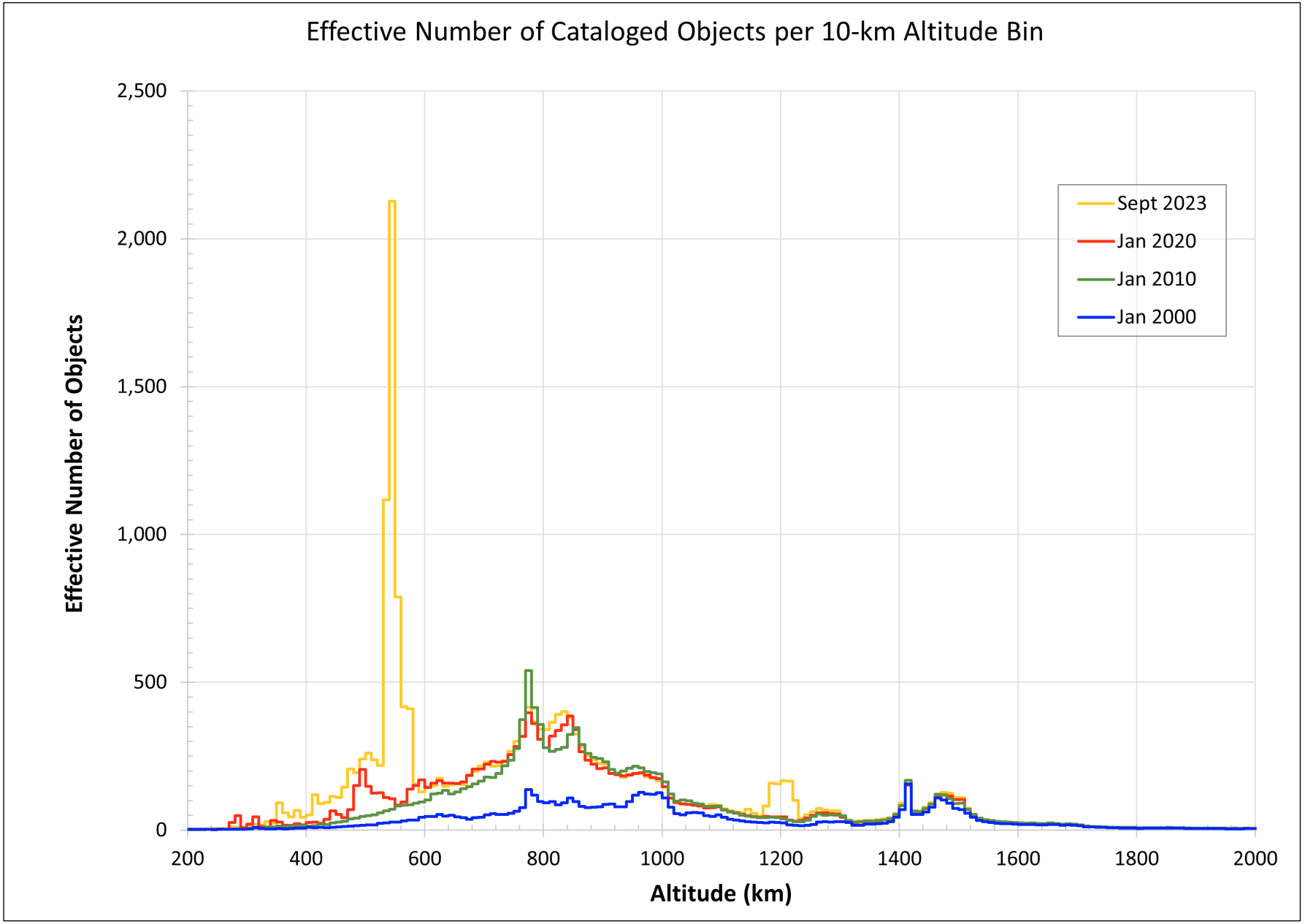

Effective numbers of objects per 10 km altitude bin between 200 and 2000 km altitude at four different epochs. These are objects, approximately 10 cm and larger, tracked by the U.S. Space Surveillance Network. The increase from 2000 to 2010 was dominated by fragments generated from the Fengyun-1C antisatellite test conducted by China in 2007 and the accidental collision between Cosmos 2251 and the operational Iridium 33 spacecraft in 2009. The increase from 2010 to 2020 was driven by the initial build-up of the Starlink large constellation (120 Starlink spacecraft were launched from May to November 2019) and by the proliferation of CubeSats below about 650 km altitude. The increase from 2020 to 2023 continues to be driven by the Starlink constellation and CubeSats below about 650 km altitude, with a new increase near 1200 km altitude driven by the OneWeb large constellation.

SATELLITE BOX SCORE

(as of 04 September 2023, cataloged by the U.S. SPACE SURVEILLANCE NETWORK)

Country/ Organization	Spacecraft*	Spent Rocket Bodies & Other Cataloged Debris	Total
CHINA	620	4399	5019
CIS	1570	5673	7243
ESA	97	35	132
FRANCE	88	533	621
INDIA	113	104	217
JAPAN	203	108	311
UK	695	1	696
USA	6734	5096	11830
OTHER	1202	84	1286
Total	11322	16033	27355

* active and defunct

Visit the NASA
Orbital Debris Program Office Website
https://orbitaldebris.jsc.nasa.gov

Technical Editor
Heather Cowardin, Ph.D.

Managing Editor
Ashley Johnson

Correspondence can be sent to:

Robert Margetta
robert.j.margetta@nasa.gov

or to:

Shaneequa Vereen
shaneequa.y.vereen@nasa.gov

National Aeronautics and Space Administration
Lyndon B. Johnson Space Center
2101 NASA Parkway
Houston, TX 77058
www.nasa.gov
https://orbitaldebris.jsc.nasa.gov/

Intl. = International; SC = Spacecraft; Alt. = Altitude; Incli. = Inclination; Addnl. = Additional; R/B = Rocket Bodies; Cat. = Cataloged
Notes: 1. Orbital elements are as of data cut-off date 30 June. 2. Additional spacecraft on a single launch may have different orbital elements. 3. Additional uncatalogued objects may be associated with a single launch.

INTERNATIONAL SPACE MISSIONS

01 July 2023 – 31 August 2023

Intl.* Designator	Spacecraft	Country/ Organization	Perigee Alt. (KM)	Apogee Alt.(KM)	Incli. (DEG)	Addnl. SC	Earth Orbital R/B	Other Cat. Debris
1998-067	ISS dispensed objects	Various	412	420	51.6	8	0	2
2023-092A	EUCLID	ESA	SUN-EARTH L2			0	0	0
2023-093A	H2SAT	GER	EN ROUTE TO GEO			0	1	1
2023-093B	SYRACUSE 4B	FR	EN ROUTE TO GEO					
2023-094A	STARLINK-5525	US	552	554	43.0	47	0	4
2023-095A	OBJECT A	PRC	1095	1123	86.5	0	1	0
2023-095B	OBJECT B	PRC	1096	1122	86.5			
2023-096A	STARLINK-30198	US	558	560	43.0	21	0	0
2023-097A	ZHUQUE-2 R/B	PRC	425	459	97.3	0	0	0
2023-098A	CHANDRAYAAN-3	IND	LUNAR SURFACE			0	1	0
2023-099A	STARLINK-6290	US	532	534	43.0	53	0	4
2023-100A	STARLING 4	US	562	584	99.5	5	2	0
2023-100G	LEO 3	CA	994	1020	99.5			
2023-101A	TIANMU-1 07	PRC	513	530	97.4	3	1	0
2023-102A	STARLINK-30240	US	552	554	43.0	14	0	0
2023-103A	OBJECT A	PRC	477	497	96.6	0	1	0
2023-103B	OBJECT B	PRC	476	493	96.6			
2023-104A	OBJECT A	PRC	481	503	97.4	0		2
2023-104B	OBJECT B	PRC	480	502	97.4			
2023-104C	OBJECT C	PRC	479	501	97.4			
2023-104D	OBJECT D	PRC	479	500	97.4			
2023-105A	STARLINK-30189	US	552	554	43.0	21	0	0
2023-106A	YAOGAN-36 05A	PRC	493	502	35.0	0	1	1
2023-106C	YAOGAN-36 05B	PRC	495	501	35.0			
2023-106E	YAOGAN-36 05C	PRC	496	500	35.0			
2023-107A	STARLINK-30165	US	553	554	43.0	21	0	0
2023-108A	JUPITER 3 (ECHOSTAR 24)	US	EN ROUTE TO GEO			0	1	0
2023-109A	DS-SAR	SING	526	530	5.0	6	0	0
2023-110A	CYGNUS NG-19	US	412	420	51.6	0	1	0
2023-111A	FENGYUN 3F	PRC	825	827	98.8	0	1	0
2023-112A	GALAXY 37	US	EN ROUTE TO GEO			0	1	0
2023-113A	STARLINK-30154	US	471	472	43.0	21	0	0
2023-114A	COSMOS 2569 (GLONASS)	CIS	19151	19175	64.8	0	1	0
2023-115A	STARLINK-30259	US	455	458	43.0	14	0	0
2023-116A	HJ-2F	PRC	484	503	97.4	0	1	3
2023-117A	OBJECT A	PRC	523	540	97.5	6	0	0
2023-118A	LUNA 25	CIS	LUNAR SURFACE			0	0	0
2023-119A	STARLINK-30166	US	426	430	43.0	21	0	0
2023-120A	LUDI TANCE-4 01A	PRC	EN ROUTE TO GEO			0	1	0
2023-121A	HEAD-3A	PRC	700	708	45.0	4	1	0
2023-122A	STARLINK-30309	US	371	373	43.0	21	0	0
2023-123A	GAOFEN 12 04	PRC	626	630	97.9	0	1	0
2023-124A	STARLINK-30267	US	509	511	53.1	20	0	0
2023-125A	PROGRESS MS-24	CIS	412	420	51.6	0	1	0
2023-126A	CAPELLA-11 (ACADIA)	US	640	649	53.0	0	2	0
2023-127A	JILIN-01 KUANFU 02A	PRC	530	547	97.6	0	0	0
2023-128A	DRAGON ENDURANCE 3	US	412	420	51.6	0	0	0
2023-129A	STARLINK-30288	US	463	465	43.0	21	0	0
2023-130A	YAOGAN-39 01A	PRC	491	501	35.0	0	1	1
2023-130B	YAOGAN-39 01B	PRC	489	502	35.0			
2023-130E	YAOGAN-39 01C	PRC	488	506	35.0			